Measurement of the $\beta - \nu$ Correlation using Magneto-optically Trapped ^{21}Na

N. D. Scielzo, S. J. Freedman, B. K. Fujikawa, and P. A. Vetter
Department of Physics, University of California at Berkeley
and Lawrence Berkeley National Laboratory, Berkeley, California 94720, USA
(Received 14 April 2004; published 30 August 2004)

The beta-neutrino correlation coefficient, $a_{\beta\nu}$, in ^{21}Na is inferred from detecting the β^+ and low-energy recoil daughter nucleus. ^{21}Na is produced at the 88-Inch Cyclotron at Lawrence Berkeley National Laboratory and 800 000 atoms are maintained in a magneto-optical trap. From the measured time of flight of recoil ions in the presence of a drift electric field, we find $a_{\beta\nu} = 0.5243 \pm 0.0091$. There may be a dependence on the trapped atom population. This and other systematic uncertainties are discussed.

DOI: 10.1103/PhysRevLett.93.102501 PACS numbers: 23.40.Bw, 23.20.En, 24.80.+y, 27.30.+t

The standard model (SM) predicts that the β decay is mediated solely by the W boson, giving rise to a pure $V - A$ Lorentz structure. The correlation of the momenta of the β and ν particles is sensitive to scalar and tensor interactions which are present in some SM extensions [1]. Experimental limits on these exotic couplings are poor, only about 10% of the dominant $V - A$ terms [2,3]. Precise measurements of this correlation are difficult because the nuclear recoil is typically <1 keV.

A precise measurement of the $\beta - \nu$ correlation coefficient, $a_{\beta\nu}$, for the ground-state mirror transition, $^{21}\mathrm{Na}(3/2^+) \rightarrow {}^{21}\mathrm{Ne}(3/2^+)$ is the focus of this work. A diagram of the β^+ decay is shown in Fig. 1. We use a magneto-optical trap (MOT) to collect and hold a pure sample of ^{21}Na atoms nearly at rest. For a source without nuclear polarization, the β decay rate is [4,5]:

$$\frac{d^3\Gamma}{dE_e d\Omega_e d\Omega_\nu} \propto F(Z, E_e) p_e E_e (E_0 - E_e)^2 \times \left[f_1(E_e) + a_{\beta\nu}(E_e) \frac{\vec{p}_e \cdot \vec{p}_\nu}{E_e E_\nu} + b_{\mathrm{Fierz}}(E_e) \frac{m_e}{E_e} \right], \quad (1)$$

where $(E_e, \vec{p}_e)$ and $(E_\nu, \vec{p}_\nu)$ are the β and ν four-momenta, E_0 is the end point energy, m_e is the electron mass, and $F(Z, E_e)$ is the Fermi function [6]. For allowed decays, f_1, $a_{\beta\nu}$, and Fierz interference term (b_{Fierz}) are functions of the fundamental weak coupling constants and nuclear matrix elements and are nearly independent of E_e. The Fermi matrix element is unity from isospin symmetry.

The Gamow-Teller contribution to the decay, λ^2, can be determined [assuming the conserved vector current (CVC) hypothesis] from the ft values of ^{21}Na and the $(0^+ \rightarrow 0^+)$ superallowed transitions as follows:

$$1 + \lambda^2 = \frac{2ft(0^+ \rightarrow 0^+)}{ft(^{21}\mathrm{Na} \rightarrow {}^{21}\mathrm{Ne})}. \quad (2)$$

For the precision necessary for this work, the ft values must be calculated to better than 1%, which requires including effects such as radiative and isospin breaking corrections. To our knowledge, the most precise calculation of this ft value to date [7] has included only some of the necessary corrections. Using this value, we find $a_{\beta\nu} = 0.558$, with an uncertainty of 0.003 based solely on the measured E_0, half-life, and branching ratio values. We estimate the net effect of the neglected corrections on the ft value of ^{21}Na to be $<0.5\%$ based on their average size for the $(0^+ \rightarrow 0^+)$ superallowed transitions [8]. We set a conservative uncertainty on $a_{\beta\nu}$ of 0.006 to account for these corrections.

To compare our results to the SM prediction, several $\sim 1\%$ E_e-dependent corrections to f_1, $a_{\beta\nu}$, and b_{Fierz} must be considered. Recoil order corrections are given in Ref. [5]. The magnetic moments of the ^{21}Na [9] and ^{21}Ne [10] nuclei determine the weak magnetism term $b = 82.6$, assuming the CVC hypothesis. The assumption of no second-class currents implies that the induced tensor term $d = 0$ for an isodoublet transition. Order-α radiative effects were included according to Ref. [11], which properly accounts for the four-body final-state from hard bremsstrahlung emission.

The ^{21}Na is produced by bombarding a powdered MgO target with 2 μA of 25 MeV protons from the 88-Inch Cyclotron at Lawrence Berkeley National Laboratory. Using the techniques described in Refs. [12,13], we maintain up to 8×10^5 ^{21}Na atoms in a MOT. The β decay leaves ^{21}Ne with a recoil of up to 230 eV in a variety of charge states [13]. Recoil ions were focused at a CsI-coated chevron microchannel plate (MCP) detector

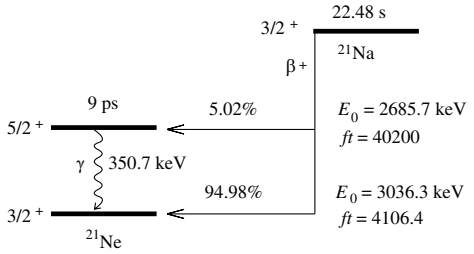

FIG. 1. β^+ decay of ^{21}Na with ft values for each branch.

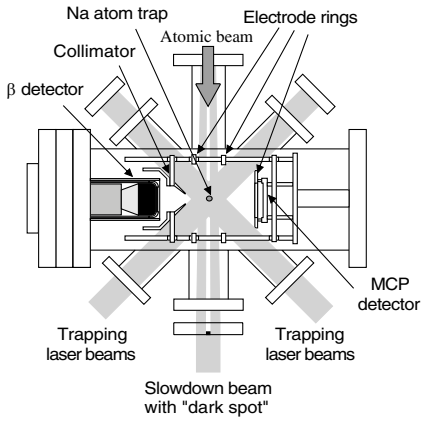

FIG. 2. Detector and electrode geometry. The scintillator for the ΔE and E components of the β detector are shown in solid black.

by a static electric field generated by a system of electrodes surrounding the trap. The electrode and detector geometry is shown in Fig. 2. The β^+s were detected in coincidence using a plastic scintillator ΔE-E β detector telescope. A nonmagnetic, tungsten-alloy collimator thick enough to stop all decay β^+s restricted the field-of-view of the β detector to a region containing the trap. The ^{21}Ne time of flight (TOF) was recorded following a trigger from either the ΔE or E detector. The $\beta - \nu$ correlation was inferred from the TOF distribution, since aligned lepton momenta result in shorter TOFs because of larger nuclear recoil towards the MCP.

A detailed Monte Carlo (MC) simulation described in [13] was necessary for interpreting the results. Decays were generated with a spatial distribution consistent with charge-coupled device (CCD) camera images of the atomic cloud. These images show an atomic cloud less than 0.5 mm from the chamber center, well described by a Gaussian distribution with a FWHM of 0.80 mm, independent of the trap population. The lepton momenta determine the recoil by momentum conservation. For β^+s that hit the β detector, the ion trajectory was calculated using SimIon 3D Version 7.0 [14]. The energy lost by the β^+ passing through a 127 μm thick Be vacuum window was calculated for each event using electron and photon transport code, EGSnrc [15]. Measured energy- and position-dependent acceptance functions for the MCP and β detectors were applied. By accepting events that deposit as little as 50 keV in the β detector, only $2.7 \pm 0.1\%$ of the spectrum is not detected. A correction is made for the true and accidental coincidences missed because only the first MCP event was accepted after each β event. A MC calculation of TOF spectrum for ground-state $^{21}Ne^{1+}$ with $a_{\beta\nu} = 1$ and $a_{\beta\nu} = 0$ is shown in Fig. 3.

Events were generated for both β decay branches, with probabilities determined by the measured branching ratios [16] after correcting for internal conversion of the

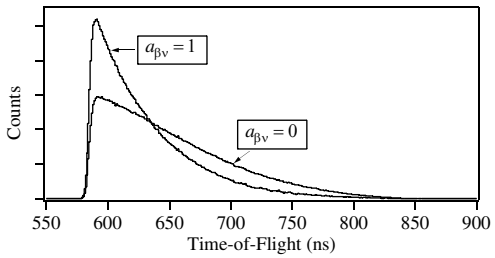

FIG. 3. Monte Carlo simulation of the time of flight spectra for $^{21}Ne^{1+}(3/2^+)$ given $a_{\beta\nu} = 1$ and $a_{\beta\nu} = 0$. There are 10^7 events in each spectrum.

excited-state γ ray [13]. Decays to the excited state have a different TOF distribution because of smaller E_0, the SM predicted $a_{\beta\nu} = -1/3$, and perturbing effect of the decay γ ray. For these decays, the $\beta - \gamma$ directional correlation, the excited-state lifetime, and the effect of recoil order and radiative corrections are negligible.

Figure 4 shows the coincident ^{21}Ne recoil time spectrum collected over 30 h. Although $\approx 80\%$ of the daughters are $^{21}Ne^0$, they provide minimal information on the $\beta - \nu$ correlation. Only $18.5 \pm 0.2\%$ of the unfocused neutrals reach the detector at energies for which the MCP detection efficiency, $\mathcal{E}_{\mathrm{MCP}}$, is energy dependent [17]. We estimate that atomic metastable $^{21}Ne^*$, for which $\mathcal{E}_{\mathrm{MCP}}$ should be nearly constant, accounts for at most 10% of the $^{21}Ne^0$ events. For $^{21}Ne^0$, we find $a_{\beta\nu} = 0.51 \pm 0.06(\mathrm{stat}) \pm 0.15(\mathrm{syst})$, where the systematic uncertainty is dominated by the detection efficiency dependence on position, angle, and energy [18].

The distance between the trap and the MCP detector is 83.08 ± 0.04 mm as determined by the arrival time of the fastest $^{21}Ne^0$ recoils. Using this distance in the MC simulation, the difference between the calculated and measured rising edge of the $^{21}Ne^{1+}$ TOF peak is 0.1 ± 0.6 ns, with the uncertainty dominated by the ± 0.1 mm uncertainty in electrode positions. This implies the magnitude of the electric field is accurate to $<0.2\%$.

The electric field collected $>99.5\%$ of the recoil ions at the MCP (in coincidence with detected β^+s). The ions were detected with nearly uniform efficiency at energies

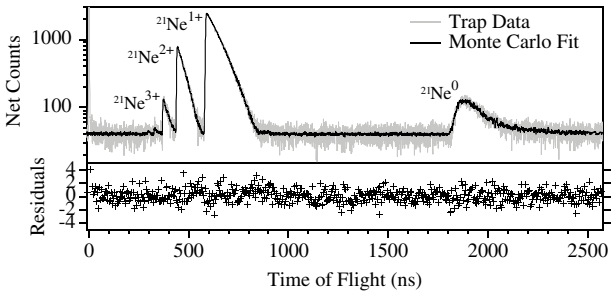

FIG. 4. Recoil ^{21}Ne spectra fit with the Monte Carlo simulation. Residuals are shown for ten bins for clarity and divided by the statistical uncertainty per bin.

of ≈ 9 keV. Recoil ions encounter no material before reaching the MCP detector and the collimator in front of the β detector suppresses most scattered β^+ backgrounds. A peak from β^+s that backscattered off the MCP and subsequently triggered the β detector was used to determine the TOF offset and implied that instrumental FWHM timing resolution was <0.9 ns.

Accidental coincidences create a flat background in the TOF spectrum. In addition, peaks every 90 ns occur from radiation emitted promptly with cyclotron proton beam bunches. They constitute 1% of all coincidences and were fit with a periodic Gaussian function and subtracted from the data shown in Fig. 4. Backgrounds from sources other than trapped atoms were measured by intentionally keeping the trap empty by blocking one of the trapping laser beams. The resulting TOF distribution was consistent with accidental coincidences.

The ΔE scintillator has a measured detection efficiency for 511 keV γ rays of $1.05 \pm 0.23\%$ and a correction for γ-^{21}Ne coincidence events must be made. The TOF distribution for these events is difficult to calculate but the events were empirically selected by requiring energy deposited in the E but not the ΔE detector. The magnitude of the spectrum was determined from the relative detection efficiency of the ΔE and E to 511 keV γ rays. The correction to the $\beta - \nu$ correlation is 0.0085 ± 0.0018.

The agreement between the measured and calculated β spectra (after accounting for the detector resolution) for $^{21}Ne^{1+}$ coincidences is shown in Fig. 5. The normalization was the only free parameter in the fit.

The shake-off ionization process can lead to systematic effects since the $\beta - \nu$ correlation was precisely measured only for daughter ^{21}Ne that have lost ≥ 2 electrons. As discussed in Ref. [13], the ratios $^{21}Ne^{2+}$:$^{21}Ne^{1+}$ and $^{21}Ne^{3+}$: $^{21}Ne^{1+}$ show no indication the β^+ or recoil ion energy influences ionization. A rough calculation indicates that the probability for electron loss for the fastest recoils could be $\sim 0.70\%$ [13] and we apply a correction to $a_{\beta\nu}$ for the possible existence of this effect.

We performed an optical rotation measurement to determine the net nuclear polarization and alignment of the trapped sodium nuclei, which if nonzero, would contribute additional correlation terms to Eq. (1). Since useful optical rotation signals required $>2 \times 10^6$ atoms, we trapped ^{23}Na using the identical trap configuration (both isotopes have spin 3/2). A 40 μW probe beam with diameter ≈ 1 mm passed through the trap 45° to the detector axis. Its polarization was oscillated from σ^+ to linear to σ^- to linear at a frequency $\omega = 50$ kHz using a photoelastic modulator. After passing through the atoms, the beam was detected using photodiodes and the absorptivity demodulated at 1ω and 2ω using a lock-in amplifier. The optical depth was determined by the DC absorption of the probe beam. The probe beam frequency was swept at 35 MHz/s through the atomic transitions of interest. Comparing the resulting line shapes to calculated line shapes for various hyperfine sublevel population distributions, we conclude that the net nuclear polarization and tensor alignment were both $<0.2\%$, independent of the trap parameters.

The free parameters in the fit to the coincident β-^{21}Ne events shown in Fig. 4 were $a_{\beta\nu}$, the number of ions in each peak, and the magnitude of the flat background. The systematic uncertainties for $^{21}Ne^{1+}$ are summarized in Table I. For higher charge states, the increased sensitivity to the background level and dead time corrections result in a larger systematic uncertainty.

For $^{21}Ne^{1+}$ recoils, we find a correlation between $a_{\beta\nu}$ and the number of trapped atoms (shown in Fig. 6) at 2.3σ. Including a linear dependence on trap population increases the confidence level in the fit to 20% from 4% for a horizontal line. We have investigated potential systematic effects which could produce a such a correlation. Gain shifts of $<1\%$ in both β and MCP detectors are the largest known population-dependent effects but account for only 6% of the observed effect. The CCD camera images and rising edge of the TOF peaks indicate the trap position was stable to <0.1 mm, regardless of trap population. The atomic cloud dimensions appear not to

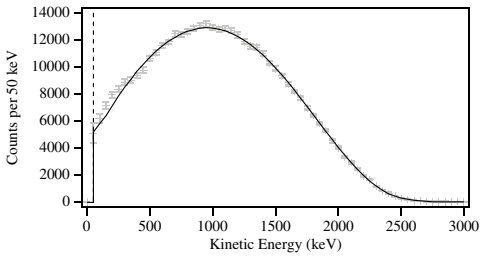

FIG. 5. The β energy spectrum for $^{21}Ne^{1+}$ with a β detector threshold at 50 keV (dashed line). Accidental and proton beam induced coincidences have been subtracted. The $\approx 1\%$ excess of counts below 300 keV is due to Compton scattering of 511 keV γ rays.

TABLE I. Corrections and systematic uncertainties.

Source	Correction	Uncertainty
Gamow-Teller branch	+0.0681	0.0018
Recoil order corrections	−0.0010	
Order-α radiative corrections	+0.0041	
Recoil ionization	−0.0033	0.0033
Polarization and alignment		0.0006
β detection		0.0024
$\mathcal{E}_{\mathrm{MCP}}$	−0.0038	0.0016
Electric field and simulation		0.0027
Annihilation γ rays	+0.0085	0.0018
β^+ scattering	+0.0039	0.0016
Background level		0.0003
Total	+0.0765	0.0060

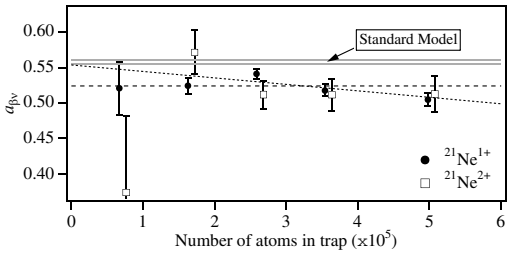

FIG. 6. $a_{\beta\nu}$ at different trap populations. The dotted line is the fit to the $^{21}Ne^{1+}$ data that depends linearly on the trap population and the dashed line is for the population-independent fit. The $^{21}Ne^{2+}$ data have been slightly offset horizontally for clarity. Error bars shown are statistical only, before readjustment by $\sqrt{\chi_r^2}$ (see text).

depend on population and cause a shift in $a_{\beta\nu}$ of <0.002 when the first 15 ns of each peak was excluded from the fit.

A possible explanation is $^{21}Na_2$ dimers formed by cold photoassociation. The MOT quadrupole magnetic field configuration can act as a magnetic trap [19] when the field gradient is large enough to support the molecules against gravity (as is the case in this work) [20]. Monte Carlo simulations that include the scattering of recoil ions off a molecular potential indicate that the largest deviations from the SM could be accounted for by a magnetically trapped $^{21}Na_2$ population of $\approx 5\%$ of the MOT population. A dimer population of this size generated by photoassociation via the MOT lasers is consistent with measured rates for Na and Cs at our MOT densities [21]. We are beginning research to quantify how many trapped molecules are present under different experimental conditions.

Extrapolating the measured $\beta - \nu$ correlation coefficients to zero trap population gives $a_{\beta\nu} = 0.551 \pm 0.013(\text{stat}) \pm 0.006(\text{syst})$, in agreement with the standard model. However, without definitive evidence of a trapped molecule population we do not make this extrapolation. Instead, we apply a procedure used by the Particle Data Group [22] to account for the spread in $^{21}Ne^{1+}$ results by scaling the statistical uncertainty by $\sqrt{\chi_r^2}$ (where the reduced chi-squared $\chi_r^2 = 2.5$ assuming no correlation with trap population). The systematic uncertainty of 0.0060 common to all $^{21}Ne^{1+}$ data remains unchanged. We find $a_{\beta\nu} = 0.5243 \pm 0.0091$ for $^{21}Ne^{1+}$, where only the total uncertainty is quoted because a simple separation of statistical and systematic uncertainties is no longer possible due to the scaling. This result deviates by 3σ from the SM calculation. A similar procedure applied to the $^{21}Ne^{2+}$ and $^{21}Ne^{3+}$ results gives $a_{\beta\nu} = 0.5207 \pm 0.0157$ and $a_{\beta\nu} = 0.564 \pm 0.068$, respectively. We find $b_{\text{Fierz}} = -0.005 \pm 0.028$ and weak magnetism $b = 59.1 \pm 26.4$ (scaled statistical uncertainties only) when these terms were independently allowed to vary along with $a_{\beta\nu}$.

We believe it is also important to accurately determine the β decay branching ratio to the first excited state of ^{21}Ne before making conclusions about the standard model. This is the largest correction applied to the data and significant discrepancies exist between measurements [23–27] that are not reflected in the currently accepted value of $5.02 \pm 0.13\%$ [16]. From the TOF spectra we can only deduce a branching ratio of $4.3 \pm 1.7\%$, with $a_{\beta\nu} = -0.17 \pm 0.28$ (scaled statistical uncertainties only) for these decays. A definitive measurement is needed to resolve this situation.

We appreciate the assistance of the technical staff at the 88-Inch Cyclotron. This work was supported by the Director, Office of Science, Office of Basic Energy Sciences, U.S. Department of Energy under Contract No. DE-AC03-76SF00098.

[1] P. Herczeg, *Precision Tests of the Standard Electroweak Model* (World Scientific, Singapore, 1995).
[2] C. H. Johnson, F. Pleasonton, and T. A. Carlson, Phys. Rev. **132**, 1149 (1963).
[3] E. G. Adelberger *et al.*, Phys. Rev. Lett. **83**, 1299 (1999).
[4] J. D. Jackson, S. B. Treiman, and H. W. Wyld, Phys. Rev. **106**, 517 (1957).
[5] B. R. Holstein, Rev. Mod. Phys. **46**, 789 (1974).
[6] H. Behrens and J. Jänecke, *Numerical Tables for Beta-Decay and Electron Capture* (Springer-Verlag, New York, 1969).
[7] O. Naviliat-Cuncic *et al.*, J. Phys. G **17**, 919 (1991).
[8] I. S. Towner and J. C. Hardy, J. Phys. G **29**, 197 (2003).
[9] O. Ames, E. A. Phillips, and S. S. Glickstein, Phys. Rev. **137**, 1157B (1965).
[10] P. Raghavan, At. Data Nucl. Data Tables **42**, 189 (1989).
[11] F. Glück, Comput. Phys. Commun. **101**, 223 (1997).
[12] M. Rowe *et al.*, Phys. Rev. A **59**, 1869 (1999).
[13] N. D. Scielzo *et al.*, Phys. Rev. A **68**, 022716 (2003).
[14] D. A. Dahl, "SimIon 3D Version 7.0, Idaho National Engineering Laboratory," 2000.
[15] I. Kawrakow, Med. Phys. **27**, 485 (2000).
[16] P. M. Endt, Nucl. Phys. A **521**, 1 (1990).
[17] B. L. Peko and T. M. Stephen, Nucl. Instrum. Methods Phys. Res., Sect. B **171**, 597 (2000).
[18] R. S. Gao *et al.*, Rev. Sci. Instrum. **55**, 1756 (1984).
[19] A. Migdall *et al.*, Phys. Rev. Lett. **54**, 2596 (1985).
[20] N. Vanhaecke *et al.*, Phys. Rev. Lett. **89**, 063001 (2002).
[21] F. K. Fatemi *et al.*, Phys. Rev. A **66**, 053401 (2002).
[22] K. Hagiwara *et al.*, Phys. Rev. D **66**, 010001 (2002).
[23] J. W. L. Talbert and M. G. Stewart, Phys. Rev. **119**, 272 (1960).
[24] S. E. Arnell and E. Wernbom, Ark. Fys. **25**, 389 (1963).
[25] D. E. Alburger, Phys. Rev. C **9**, 991 (1974).
[26] G. Azuelos, J. E. Kitching, and K. Ramavataram, Phys. Rev. C **15**, 1847 (1977).
[27] H. S. Wilson, R. W. Kavanagh, and F. M. Mann, Phys. Rev. C **22**, 1696 (1980).